2013 IEEE/RSJ International Conference on
Intelligent Robots and Systems (IROS)
November 3-7, 2013. Tokyo, Japan

Teleoperated Control based on Virtual Fixtures for a Redundant Surgical System

Edoardo Lopez, Loredana Zollo and Eugenio Guglielmelli

Abstract— **One of the main limitations of systems for Minimally Invasive Robotic Surgery is the lack of haptic feedback. In this paper, a teleoperated system for robotic surgery is introduced, able to guide the surgeon towards a target anatomy by providing her with force feedback based on Virtual Fixtures (VF). The teleoperated system has a redundant slave robot. A closed-form inverse kinematics is proposed to solve redundancy that is based on an optimization approach in one variable. Four different cost objective functions are proposed in the paper and one is implemented and validated, i.e. the cost function aimed at minimizing the amount of space of the robot in the operative theater during the surgical procedure. The proposed teleoperated architecture has been tested on a teleoperated system composed of a 3-DoFs haptic joystick and a 7-DoFs anthropomorphic manipulator. Experimental tests on 12 volunteer subjects have been carried out. Results demonstrate that a force feedback based on VF provides a statistically significant enhancement of procedure accuracy.**

I. Introduction

Robots for Computer Assisted Surgery (CAS) can be distinguished in *active* robots, which perform the operation autonomously on the basis of pre-operative planning, and *semi-active* robots, which require the surgeon to command the motion of the laparoscopic instrument connected to the manipulator. Semi-active systems represent nowadays the dominant paradigm of robots for teleoperated Minimally Invasive Robotic Surgery (MIRS). In a teleoperated approach the surgeon interacts with a master interface; his/her movements are mapped into the movements of another manipulator (i.e. the slave robot), which interacts with patient's tissues. Teleoperated robotic systems can be notably beneficial for a number of reasons, e.g. (i) they can increase surgeon's ability to perform operations in laparoscopy with respect to the traditional approach since the hand-eye coordination might be restored using ergonomic consoles and the stereo-vision can increase depth perception; (ii) the dexterity during intervention can be improved by designing customized articulated or flexible laparoscopic instruments that provide additional intra-corporeal degrees of freedom (DoFs); (iii) the pivoting effect caused by the incision point that acts as a Remote Center of Motion (RCM) can be automatically compensated.

This work was supported by by the national project PRIN 2010 "HANDBOT - Biomechatronic Hand Prostheses Endowed with Bio-inspired Tactile Perception, Bi-directional Neural Interfaces and Distributed Sensory-motor Control", CUP: B81J12002680008, and "ITINERIS 2" on the technological transfer, CUP: F87G10000130009. Edoardo Lopez, Loredana Zollo and Eugenio Guglielmelli are with the Laboratory of Biomedical Robotics and Biomicrosystems, Universita' Campus Bio-Medico di Roma, Via Alvaro del Portillo, 21 - 00128 Rome, Italy (email: e.lopez@unicampus.it).

Commercial solutions extensively used in surgery, such as *Da Vinci* or *Zeus* systems, still do not provide surgeons with haptic feedback; the absence of kinesthetic as well as tactile feedback is recognized as one of the major drawbacks of these systems [1], [2]. Haptic feedback is generally aimed at providing the user with proprioceptive and/or tactile sensations representing the interaction with patient's tissues, i.e. information about the hardness of tissues and the surface morphology and roughness. However, interaction forces have to be measured by means of a force sensor on the tip of the laparoscopic instrument in order to provide an affordable measure of the interaction. Nowadays, there are no commercial sensors addressing the requirements of sterilizability, biocompatibility and miniaturization and able to provide both forces and torques [3]. Moreover, the integration of these force sensors in disposable or semi-disposable instruments increases the surgical operation total cost.

The absence of force sensors compatible with MIRS requirements represents the main bottleneck for providing kinestetic feedback on the interaction forces with patient's tissues; nevertheless, users can be given haptic feedback not representative of such interactions, but aimed at guiding them towards a predefined target [4]–[7], or at preventing them from penetrating in undesired regions [7]–[10]. This process is generally referred to as *Virtual Fixtures* (VF).

It is worth noticing that high update rate is required in order to provide users with effective haptic feedback [11]. Hence, computational expensive processes should be avoided. When considering redundant manipulators, on-line evaluation of inverse kinematics by means of iterative approaches, such as iterative algorithms based on the pseudo-inverse Jacobian matrix, may lead to high computational burden and, consequently, low update rate, unless complex and expensive solutions, such as non-linear parallel solvers, are used. Kapoor *et al.* introduced an optimization-based approach to provide the surgeon with VF, able to solve the inverse kinematics in 5 to 50 iterations [7]. However, the system update-rate was equal to 30 ms, still too low for good-quality haptic feedback. This technique has been recently used to control a teleoperated system during knotting, with a maximum update rate of 10 ms [10]. Alternatively, closed-form inverse kinematics can be formulated, although it should be defined specifically for each manipulator.

In this paper, a novel approach of teleoperated control based on VF is presented for a robotic system for surgery characterized by an anthropomorphic redundant slave manipulator. VF are proposed to guide surgeon's motion towards a target anatomy. Compared with other approaches:

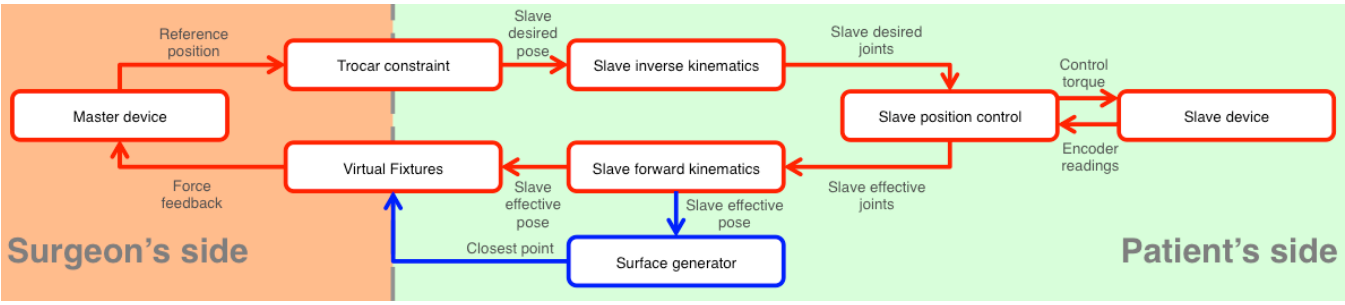

Fig. 1. Structure of the control system. Red elements are guaranteed to be processed in real-time, whereas blue elements are updated as fast as possible with no fixed cycle times.

- Force feedback provided by means of VF is guaranteed to be smooth and C^1 continuous, thus avoiding abrupt changes; moreover, force feedback can be limited only to a region close enough to the target anatomy;
- In spite of slave redundancy, heavy computational processes are avoided through a closed-form inverse kinematics, and optimised robot behaviours are implemented. Inverse kinematics of slave manipulator is solved with an optimization-based approach in only one variable, whereas traditional inverse kinematics iterative algorithms generally present a number of variables equal to the number of DoFs of the manipulator; moreover, computation of pseudo-inverse of Jacobian matrix is avoided;
- Safety has been regarded as one of main requirements for the proposed setup. Slave manipulator may present high joints velocity and unpredictable behavior close to singular configurations; thus, strategies for avoiding singular configurations are presented and implemented; this safety feature is generally not explicitly considered in current research works [7], [10];
- The overall amount of space of the slave manipulator in the operating theater is minimized, in order to ease access to the operating table for personnel, such as scrub nurses or other surgeons. This objective is achieved by formulating a cost function to optimize the inverse kinematics.

In conclusion, the proposed system introduces force feedback to enhance surgical performance, without measuring the interaction forces with patient's tissues. Expedients to guarantee hard real-time and fast update-rate are considered, formulating a closed-form inverse kinematics for the redundant slave manipulator and selecting a target anatomy reconstruction technique presenting advantages over other methods, as explained in Subsect. II-D.

The paper is structured as follows. Section II presents the proposed control architecture for the teleoperated system. Section III presents how singular configurations can be avoided. Experimental setup and protocol are described in Sect. IV, and results are reported in Sect. V. Finally, Sect. VI presents conclusion and the next step of this research.

II. Teleoperated Control Architecture with Virtual Fixtures

An overview of the proposed teleoperated architecture is presented in Fig. 1. Surgeon interacts with the *master device* in order to provide the reference position for the slave manipulator, defining the position of the laparoscopic instrument distal tip. However, he/she cannot define autonomously the orientation of the surgical instrument, which is instead constrained by the trocar position, i.e. the position of the incision point on the patient's skin, and it is evaluated by block *trocar constraints* (Subsect. II-B).

The pose of the slave device, in terms of laparoscopic instrument orientation and distal extremity position, is provided as input to the block named *slave inverse kinematics*, which calculates the corresponding desired joints configuration. Redundancy can be exploited to satisfy a number of secondary objectives, as explained in Subsect. II-C; singular configurations are avoided as shown in Sect. III. Desired joint configuration represents the input for the *slave position control*, which defines the appropriate control torque for the *slave device*. Accurate positioning can be reached by means of several control architectures [13]–[15].

Block *slave position control* provides also the effective joints measurement to the block named *slave forward kinematics*, which evaluates the effective pose in the Cartesian space of the slave device. A proper feedback force is then defined by the block called *virtual fixtures* in order to guide the surgeon towards the target anatomy. Knowledge about the closest point to the instrument tip on the target surface is required. Closest point is evaluated by the *surface generator*. Eventually, feedback force is applied to the surgeon's hand by the master device.

Each block is in-depth described in the following Subsections.

A. Master device

User interacts with the master device to set intra-corporeal position $\boldsymbol{P_E}$ for the slave manipulator. The master device exerts on the user hand the feedback force, which is evaluated in Subsect. II-D. User sets also rotation angle ψ around the laparoscopic instrument axis.

B. Trocar constraint

Trocar position constraints the orientation of the laparoscopic instrument, in order to ensure the instrument to pass through the incision point. Instrument axis (axis $\boldsymbol{z_7}$ in Fig. 2) has to pass through the trocar position and the desired laparoscopic instrument distal extremity $\boldsymbol{P_E}$. Thus,

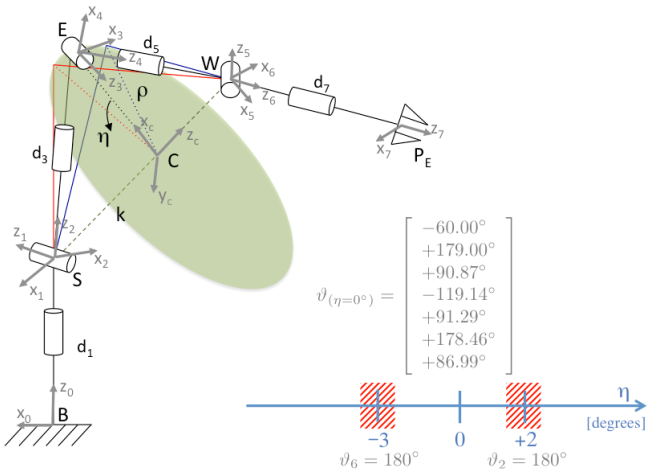

Fig. 2. Structure of the anthropomorphic manipulator. Redundancy enables elbow $\boldsymbol{E}$ to move along the green circumference. Two singular configurations are shown in the picture (red and blue configurations).

the homogeneous transformation matrix ${}^{0}\boldsymbol{T}_{\boldsymbol{P_E}}$ describing the desired pose of the laparoscopic instrument is given by

$$ {}^{0}\boldsymbol{T}_{\boldsymbol{P_E}} = \begin{bmatrix} \boldsymbol{R_a}(\alpha)\boldsymbol{R_z}(\psi) & \lambda_p \boldsymbol{P_E} \\ 0 \quad 0 \quad 0 & 1 \end{bmatrix} \tag{1} $$

where λ_p is an arbitrarily chosen scaling factor; $\boldsymbol{R_z}(\psi)$ is the rotation matrix related to a rotation of angle ψ around laparoscopic instrument $\boldsymbol{z_7}$ axis; $\boldsymbol{R_a}(\alpha)$ is the rotation matrix of angle α around axis $\boldsymbol{a}$, being $\alpha = \text{atan2}\left(\|\boldsymbol{z_0} \times \boldsymbol{z_7}\|, \boldsymbol{z_0}^T \boldsymbol{z_7}\right)$ the angle between axis $\boldsymbol{z_0}$ and axis $\boldsymbol{z_7}$, and $\boldsymbol{a} = (\boldsymbol{z_0} \times \boldsymbol{z_7}) / \|\boldsymbol{z_0} \times \boldsymbol{z_7}\|$ the axis perpendicular to both $\boldsymbol{z_0}$ and $\boldsymbol{z_7}$.

C. Slave robot inverse kinematics

The slave robot is supposed to be an anthropomorphic redundant manipulator, as shown in Fig. 2. For it a closed-form inverse kinematics can be evaluated, once the elbow position $\boldsymbol{E}$ has been defined [12]. Due to the anthropomorphic structure of the robot, for a pre-defined end-effector pose, $\boldsymbol{E}$ can only rotate around a circumference perpendicular to axis $\boldsymbol{z_c}$ connecting the shoulder $\boldsymbol{S}$ with the wrist $\boldsymbol{W}$. Thus, redundancy can be analyzed by introducing a further parameter η, which represents the angular rotation of point $\boldsymbol{E}$ around the axis $\boldsymbol{z_c}$. Hence, the solution space $\boldsymbol{E}(\eta) \in [-\pi, \pi]$ for the elbow position is represented by

$$ \boldsymbol{E}(\eta) = \boldsymbol{C} + \rho \left[\boldsymbol{x_c}, \boldsymbol{y_c}, \boldsymbol{z_c}\right] \left[\cos(\eta), \sin(\eta), 0\right]^T \tag{2} $$

where $\boldsymbol{x_c}$ is the unit vector within the circumference plain pointing towards the previous elbow position, $\boldsymbol{y_c}$ is the unit vector perpendicular to both $\boldsymbol{x_c}$ and $\boldsymbol{z_c}$, $\boldsymbol{C}$ and ρ are, respectively, the center and the radius of the circumference, they are given by

$$ \begin{aligned} \boldsymbol{C} &= \boldsymbol{S} + k\boldsymbol{z_c} \\ \rho &= \sqrt{d_3^2 - k^2} \end{aligned} \qquad k = \frac{\|S-W\|^2 + d_3^2 - d_5^2}{2\|S-W\|} \tag{3} $$

where k is the distance between vertex $\boldsymbol{S}$ and foot of the altitude $\boldsymbol{C}$ of triangle identified by points $\boldsymbol{S}$, $\boldsymbol{E}$ and $\boldsymbol{W}$, and ρ is its altitude. Elbow position $\boldsymbol{E}$ can be the result of an optimization process aimed at optimizing a target function (as for instance in [13]).

Knowledge about position of $\boldsymbol{E}$ is required to analytically solve the inverse kinematics; joints 1–3 are the Euler angles equivalent to the rotation matrix $\boldsymbol{R_E} = [(\boldsymbol{z_3} \times \boldsymbol{x_4}), \boldsymbol{z_3}, \boldsymbol{x_4}]$, where $\boldsymbol{x_4}$ is directed as the vector connecting shoulder $\boldsymbol{S}$ and elbow $\boldsymbol{E}$, and $\boldsymbol{z_3}$ is perpendicular to both $\boldsymbol{x_4}$ and the axis connecting elbow $\boldsymbol{E}$ and wrist $\boldsymbol{W}$. Joint 4 is equal to

$$ \vartheta_4 = \text{acos}\left[\left(d_3^2 + d_5^2 - \|\boldsymbol{W} - \boldsymbol{S}\|^2\right) / \left(2 d_3 d_5\right)\right] \in [0; \pi] \tag{4} $$

by cosine theorem applied to triangle $\boldsymbol{S}$, $\boldsymbol{E}$ and $\boldsymbol{W}$; whereas joints 5–7 are the Euler angles equivalent to the rotation matrix ${}^{4}\boldsymbol{R}_{\boldsymbol{P_E}} = ({}^{0}\boldsymbol{R}_4)^{T\,0}\boldsymbol{R}_{\boldsymbol{P_E}}$, where matrix ${}^{0}\boldsymbol{R}_4$ can be calculated once joints 1–4 have been evaluated, and matrix ${}^{0}\boldsymbol{R}_{\boldsymbol{P_E}}$ is the rotation matrix corresponding to the homogeneous transformation matrix (1).

A number of target functions $w(\eta)$ can be formulated to define the optimal value η^* and, consequently, the optimal elbow position $\boldsymbol{E}(\eta^*)$. Four possible target functions are proposed in the following, all potentially adequate for a surgical teleoperated scenario. They are

$$ w(\eta) = \sum_{i=1}^{7} \frac{\dot{\vartheta}_i^2(\eta)}{\dot{\vartheta}_{i,M}^2} \tag{5} $$

$$ w(\eta) = \sum_{i=1}^{7} \frac{(\vartheta_i(\eta) - \hat{\vartheta}_i)^2}{(\vartheta_{i,M} - \vartheta_{i,m})^2} \tag{6} $$

$$ w(\eta) = \|\boldsymbol{E}(\eta) - \hat{\boldsymbol{E}}\|^2 \tag{7} $$

$$ w(\eta) = \sum_{j=1}^{m} \frac{1}{\|\boldsymbol{E}(\eta) - \hat{\boldsymbol{P}}_{\boldsymbol{O,j}}\|^2} \tag{8} $$

where $\dot{\vartheta}_{i,M}$ is the maximum velocity of joint i; $\hat{\vartheta}_i$, $\vartheta_{i,M}$ and $\vartheta_{i,m}$ are, respectively, the central, the maximum and the minimum value of the variation range of joint i; $\hat{\boldsymbol{E}}$ is an arbitrarily chosen attractor point; $\hat{\boldsymbol{P}}_{\boldsymbol{O,j}}$ is the Cartesian position of obstacle j ($m \geq 1$ obstacles are considered).

Cost function (5) tries to reduce joint velocity, thus enhancing system safety; function (6) is aimed at increasing the distance from mechanical joint limits; function (7) attempts to keep the elbow position close to a defined point in the space $\hat{\boldsymbol{E}}$; function (8) is aimed at increasing the distance from a number $m \geq 1$ of obstacles. Observe that, for function (7), if point $\hat{\boldsymbol{E}}$ is chosen on $\boldsymbol{z_0}$ axis, the overall amount of space occupied by the robot in the $\boldsymbol{x_0 y_0}$ plane, i.e. the floor plane, can be minimized.

In order to increase system safety, avoiding singular configurations, constraints can be applied to the optimization approach, as explained in Sect. III.

D. Virtual Fixtures and Surface generation

Force feedback based on VF has been been implemented to guide user's movement towards a target anatomy. Knowledge about the target anatomy has to be acquired, since VF are evaluated on the basis of the position of the laparoscopic instrument distal tip and this a priori knowledge. The eABOS method has been exploited to acquire such an information [16]. This method has been chosen for three main reasons:

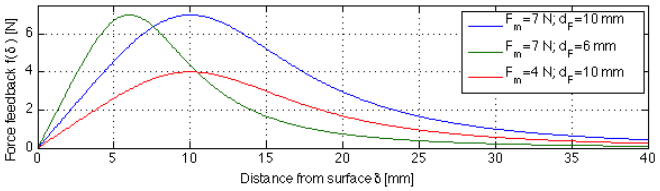

Fig. 3. Feedback force profile varying with the distance from the reconstructed surface. It is shown for three different couples of parameters F_m and d_F.

(i) surface is reconstructed from a set of not ordered control points taken on the target anatomy; (ii) reconstructed surface is saved as a 2D struct; moreover, neighboring points on the surface are neighboring elements in the 2D grid, thus simplifying the search for the nearest point to an element moving smoothly close to the reconstructed surface; (iii) C^1 continuity of surface can be guaranteed. Moreover, points outside from the convex hull of the control points acquired on the target anatomy can be rejected, so that boundary of the reconstructed surface corresponds to the boundary of the target region, if it is convex.

Feedback force is provided to guide the user towards the point on the reconstructed surface that is closest to the laparoscopic instrument distal extremity. Thus, feedback force direction is defined by the vector connecting the effective instrument distal extremity position to the closest point on the surface, which has to be real-time evaluated. Search for the closest point on a surface is generally computationally expensive and time consuming. In order to reduce the computational burden, search can be limited to the neighbor of the previously evaluated closest point, thus limiting the search process to a small part of the 2D struct.

On the other hand, feedback force magnitude should vary according to the distance from the closest point to the surface. Observe that force feedback should be used only if the user is quite close to the target anatomy surface. It has to be disabled if the user is very far from the surface; in fact, in this case it is reasonable to assume that the user is able to move autonomously and does not need assistance towards the surface. Hence, an *attraction limit* distance d_F value has to be defined. Thus, relationship between feedback force magnitude and distance should: (i) increase approximately linearly if the distance is lower than a threshold value d_F; (ii) be upper-limited to a maximum feedback force value F_m; (iii) decrease down to zero if the distance is greater than d_F; (iv) be C^1 continuous, in order to avoid abrupt changes. To satisfy such requirements, the following relationship has been defined

$$f(\delta) = \frac{4d_F^3 F_m \delta}{3d_F^4 + \delta^4} \tag{9}$$

where δ is the distance from the surface. Feedback force is reduced at 10% of F_m for $\delta \approx 3.4 d_F$. Profiles for several couples of values F_m and d_F are shown in Fig. 3.

It is worth noticing that in the proposed setup, the user actively controls the position of the distal extremity of the instrument through a 3-DoFs device, whilst orientation is automatically controlled (as explained in Subsect. II-B). She/he receives only a 3-DoFs force feedback. Therefore, there is correspondence between controlled DoFs and force feedback, and sensor/actuator asymmetries (which can lead to stability problems [17]) are avoided.

III. Safety Measures

As discussed in Subsect. II-C, joints $[\vartheta_1; \vartheta_2; \vartheta_3]$ and $[\vartheta_5; \vartheta_6; \vartheta_7]$ can be regarded as two spherical wrists.

Thus, kinematic singularities are obtained for $\vartheta_{2,6} = 0, \pi$. For $\vartheta_2 = \pi$, base $\boldsymbol{B}$, shoulder $\boldsymbol{S}$ and elbow $\boldsymbol{E}$ are aligned (red configuration in Fig. 2); similarly, for $\vartheta_6 = \pi$ end-effector position $\boldsymbol{P_E}$, wrist $\boldsymbol{W}$ and elbow $\boldsymbol{E}$ are aligned (blue configuration in Fig. 2):

$$\boldsymbol{E}_{(\vartheta_2=\pi)} = \boldsymbol{B} + (d_1 + d_3)\boldsymbol{z_0} \tag{10}$$
$$\boldsymbol{E}_{(\vartheta_6=\pi)} = \boldsymbol{P_E} - (d_5 + d_7)\boldsymbol{z_7} \tag{11}$$

Cases $\vartheta_{2,6} = 0$ are not considered since these values are outside from robot mechanical joint limits. On the other hand, points $\boldsymbol{E}_{(\vartheta_2=\pi)}$ and $\boldsymbol{E}_{(\vartheta_6=\pi)}$ lie on the green circumference in Fig. 2 representing the possible elbow positions compatible with the desired end-effector pose only if following conditions are satisfied

$$\left\|\boldsymbol{E}_{(\vartheta_2=\pi)} - \boldsymbol{W}\right\| = d_5 \qquad \left\|\boldsymbol{E}_{(\vartheta_6=\pi)} - \boldsymbol{S}\right\| = d_3 \tag{12}$$

In such a case, angles $\eta_2 : \boldsymbol{E}(\eta_2) = \boldsymbol{E}_{(\vartheta_2=\pi)}$ and $\eta_6 : \boldsymbol{E}(\eta_6) = \boldsymbol{E}_{(\vartheta_6=\pi)}$ can be evaluated and excluded from the possible solution space of angular variable η. Thus, the provided values $\eta \neq \eta_2$ and $\eta \neq \eta_6$ can be used as constraints for the optimization problem, as explained in Subsect. II-C.

In order to avoid also configurations close to singular ones, criteria (12) can be modified into:

$$\left|\left\|(d_1 + d_3)\boldsymbol{z_0} + d_7\boldsymbol{z_7} + \boldsymbol{B} - \boldsymbol{P_E}\right\| - d_5\right| \leq \varepsilon_l \tag{13}$$
$$\left|\left\|d_1\boldsymbol{z_0} + (d_5 + d_7)\boldsymbol{z_7} + \boldsymbol{B} - \boldsymbol{P_E}\right\| - d_3\right| \leq \varepsilon_l \tag{14}$$

being ε_l a threshold value, $\boldsymbol{S} = \boldsymbol{B} + d_1\boldsymbol{z_0}$ and $\boldsymbol{W} = \boldsymbol{P_E} - d_5\boldsymbol{z_7}$. Finally, in order to ensure $|\vartheta_{2,6} - \pi| > \epsilon_\vartheta$, being ε_ϑ a threshold value, constraints can be modified into:

$$\eta_2 - \frac{d_3}{\rho}\varepsilon_\vartheta < \eta < \eta_2 + \frac{d_3}{\rho}\varepsilon_\vartheta \tag{15}$$

$$\eta_6 - \frac{d_5}{\rho}\varepsilon_\vartheta < \eta < \eta_6 + \frac{d_5}{\rho}\varepsilon_\vartheta \tag{16}$$

being ρ the radius of circumference in Fig. 2.

IV. Experimental Setup

In order to test the proposed system, an abdominal surgery setup has been reproduced, as shown in Fig. 4. The teleoperated robotic system consists of the Novint Falcon haptic joystick as master and the Kuka Light Weight Robot 4+ (LWR) as slave. An aluminum bar (diameter: 12.8 mm, length: 600 mm) has been attached to the end-effector of LWR to mimic a laparoscopic instrument. An elastic tissue (95% polyamide, 7% elastan) has been strengthened on the transverse plane of the abdominal cavity, approximately at the kidney height. Cavity has been accessed by a hole in the abdomen of a male body phantom made of hard plastic. Scene has been recorded by a camera (640x480 pixels).

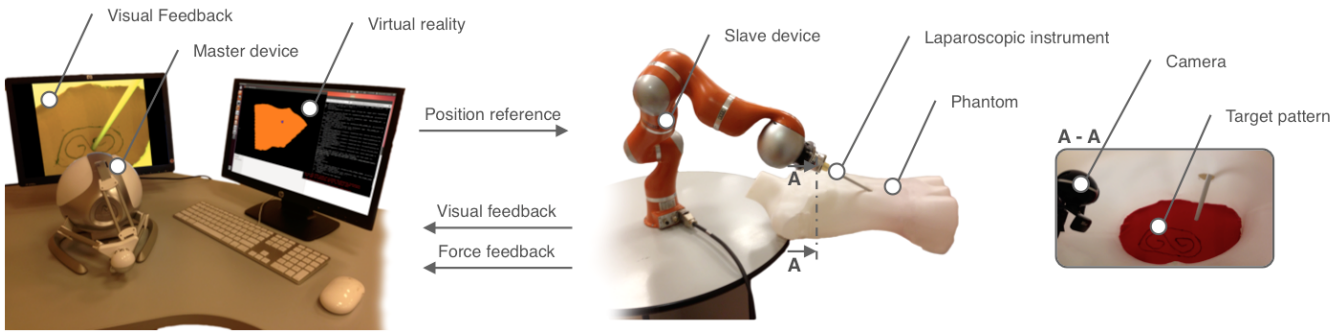

Fig. 4. User interacts with the master device to provide a reference position for the slave device, which maneuvers the laparoscopic instrument. The laparoscopic instrument is inserted within the abdominal cavity of a phantom. The user has to follow a target path drawn on a compliant tissue. Scene is acquired through a camera. System provides the user with visual feedback, acquired by the camera, and VF.

User has been provided with a visual feedback from the 2D camera and with a virtual reality scene, where the laparoscopic instrument distal extremity position is shown with respect to the reconstructed surface. Surface has been reconstructed from 33 predefined control points. No 3D vision has been involved.

System has been controlled by a 1.6 GHz PC - 4 GB DDR3 RAM. Real-time is guaranteed by a Xenomai-patched kernel (www.xenomai.org); software modules have been implemented in the OROCOS and ROS frameworks (www.orocos.org, www.ros.org). Position of LWR has been accurately controlled by the robot embedded position control [18]. Reference joint vector has been updated at 250 Hz.

For the experimental validation, twelve healthy subjects have been enrolled. They have been randomly divided into two groups. First group has not been provided with force feedback; second group has been provided with the force feedback generated with VF, as explained in Subsect. II-D. Parameters F_m and d_F have been set equal to $4\ N$ and $40\ mm$, respectively. Subjects have been given the possibility to familiarize with the setup, trying to move the instrument on the target anatomy and to follow the path shown in Fig. 4 for three times maximum. Then, they have been asked to follow the path and their motion has been recorded.

For solving redundancy, the optimization of cost function (7) has been carried out with the Nelder Mead Simplex Method. It corresponds to minimize the amount of space of the robot in the operating room floor.

V. Results

An example of trajectory followed by a user guided by VF is shown in Fig. 5; the feedback force varying with the distance from the target anatomy is also shown. Maximum force exerted on the subjects has been equal to 3.15 N.

In order to evaluate performance achieved by the subjects involved in the experiment, two indicators have been chosen: distance from the path (i.e. average distance between the laparoscopic instrument distal tip and the closest point on the path during the test) and distance from the surface (i.e. average distance between the laparoscopic instrument distal tip and the closest point within the surface during the test). Results are reported in Tab. I.

Performance enhancement in reducing the distance from the surface is highly statistically significant, and distance is reduced to almost one third when force feedback is applied (enhancement equal to 175.5%). Considering the distance from the path, statistically significance is borderline (p-value $= 0.065$). It is worth noticing that the force feedback is aimed to reduce the distance from the surface, and only indirectly the distance form the path. However, it is expected that this enhancement could become statistically significant enrolling more subjects to validate the setup.

Task execution time is approximately equivalent for both groups (i.e. 66 s for group not receiving feedback, 65.5 s for group receiving VF, p-value > 0.95).

In order to evaluate whether the proposed cost function (7) can effectively minimize the amount of space of the slave manipulator, trajectory of one user has been recorded and joint vector for the slave manipulator has been evaluated three times, varying the cost function, as shown in Fig. 6. Results are quoted in Tab. II. Area covered by the elbow $\boldsymbol{E}$ in the $\boldsymbol{x_0 y_0}$ plane during the motion of the robot is highly

TABLE I

Enhancement in performances due to haptic feedback

	Distance from path		Distance from surface	
	w/ feedb.	w/o feedb.	w/ feedb.	w/o feedb.
Mean [mm]	13.0	21.0	6.9	19.0
St.err. [mm]	5.5	3.8	1.2	3.6
p-value	0.065		0.019	
Enhancement	61.1%		175.7%	

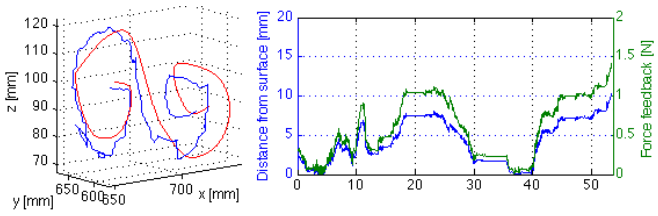

Fig. 5. Example of trajectory (left; blue: user trajectory, red: reference trajectory) and force feedback provided to the subject as a function of the distance between the instrument distal extremity and the surface (right).

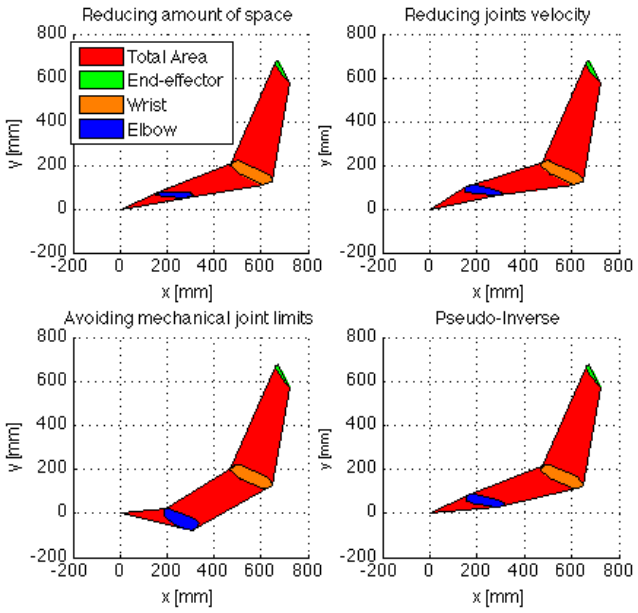

Fig. 6. Overall amount of space occupied by the slave manipulator during the task in the operating theater. Different optimization strategies have been compared: (top-left) minimization of the amount of space, (top-right) minimization of joint velocity, (bottom-left) maximization of the distance from the joint limits. Finally, (bottom-right) the case of inverse kinematics based on the Jacobian pseudo-inverse matrix is shown.

TABLE II

AMOUNT OF SURFACE OCCUPIED BY THE SLAVE MANIPULATOR

	Minimizing amount of space	Reducing joints velocity	Avoiding joint limits	Pseudo-inverse
Elbow	$-$ $29.4cm^2$	$+53.3\%$ $45.0cm^2$	$+175.8\%$ $80.9cm^2$	$+93.8\%$ $56.9cm^2$
Total	$-$ $1083.5cm^2$	$+4.4\%$ $1130.8cm^2$	$+24.8\%$ $1352.3cm^2$	$+9.8\%$ $1189.7cm^2$

reduced with the cost function (7). Considering the total area occupied by the robot on the operating theater floor, the area is still reduced. However, percent variation is lower, since position of wrist $\boldsymbol{W}$ and end-effector $\boldsymbol{P_E}$ are not affected by the chosen cost function. Results obtained are highly dependent on the initial joint vector, which has been chosen to be the same in all four executions.

Hard real-time has been guaranteed at 250 Hz[1]. Bottleneck to faster update rates is not caused by inverse kinematics (which can be cycled up to 2.94 kHz, whereas update rate has been limited to 750 Hz using iterative approaches and to 111 Hz using the approach proposed by Kapoor *et al.* [7]), but by the update-rate of master and slave devices.

VI. CONCLUSIONS AND FUTURE WORKS

In this paper a teleoperated system for robotic surgery has been proposed, able to provide the surgeon with force feedback based on VF in order to guide him/her towards a target surface. A novel closed-form inverse kinematics for a redundant slave manipulator has been presented, aimed at reducing system computational burden. Four optimization criteria have been presented to handle redundancy.

The proposed control architecture has been implemented on a hard real-time architecture and tested on twelve volunteer subjects. Experimental tests demonstrated the efficacy of force feedback to guide user's movements, able to reduce to almost one third the distance between the laparoscopic instrument position and the target anatomy. Redundancy has been exploited to effectively minimize the amount of space of the robot in the operative theater while moving.

In order to complete the validation of the proposed setup, subject tests involving surgeons experts in robotic-aided surgery are envisaged. Moreover, automatic surface reconstruction technique, capable of defining the target surface from the endoscopic images, should be considered for simplifying translation to clinical practice.

[1]Real-time is guaranteed for at least 99% of instances.

REFERENCES

[1] F. W. Mohr, V. Falk, A. Diegeler, *et al.*, "Computer-enhanced "robotic" cardiac surgery: Experience in 148 patients," *J. Thorac. Cardiovasc. Surg.*, vol. 121, no. 5, pp. 842–853, 2001.

[2] B. Bethea, A. M. Okamura, M. Kitagawa, *et al.*, "Application of haptic feedback to robotic surgery," *J. Laparoendosc. Adv. S.*, vol. 14, no. 3, pp. 191–195, 2004.

[3] A. L. Trejos, R. V. Patel, and M. D. Naish, "Force sensing and its application in minimally invasive surgery and therapy: a survey," *Proc. Inst. Mech. Eng. C J. Mech. Eng. Sci.*, vol. 224, no. C7, pp. 1435–1454, 2010.

[4] S. C. Ho, R. D. Hibberd, and B. L. Davies, "Robot assisted knee surgery," *IEEE Eng. Med. Biol.*, vol. 14, no. 3, pp. 292–300, 1995.

[5] M. Li, M. Ishii, and R. H. Taylor, "Spatial Motion Constraints Using Virtual Fixtures Generated by Anatomy," *IEEE Trans. Robot.*, vol. 23, no. 1, pp. 4–19, 2007.

[6] J. Ren, R. V. Patel, K. A. McIsaac, *et al.*, "Dynamic 3-D Virtual Fixtures for Minimally Invasive Beating Heart Procedures," *IEEE Trans. Med. Imag.*, vol. 27, no. 8, pp. 1061–1070, 2008.

[7] A. Kapoor, M. Li, R. H. Taylor, "Constrained Control for Surgical Assistant Robots," *IEEE ICRA 2006*, 2006, pp. 231-236

[8] A. Bettini, P. Marayong, S. Lang, *et al.*, "Vision-assisted control for manipulation using virtual fixtures," *IEEE Trans. Robot.*, vol. 20, no. 6, pp. 953–966, 2004.

[9] K. W. Kwok, G. P. Mylonas, L. W. Sun, *et al.*, "Dynamic Active Constraints for Hyper-Redundant Flexible Robots," in *Miccai 2009*, pp. 410–417, 2009.

[10] T. Xia, A. Kapoor, P. Kazanzides and R. Taylor, "A constrained optimization approach to virtual fixtures for multi-robot collaborative teleoperation," *IEEE/RSJ IROS 2011*, 2011, pp. 639–644.

[11] S. Choi and H. Z. Tan, "Effect of update rate on perceived instability of virtual haptic texture," *IEEE/RSJ IROS 2004*, 2004, pp. 3577–3582.

[12] D. Tolani, A. Goswami, and N. I. Badler, "Real-Time Inverse Kinematics Techniques for Anthropomorphic Limbs," *Graphical Models*, vol. 62, no. 5, pp. 353–388, 2000.

[13] L. Zollo, B. Siciliano, C. Laschi, *et al.*, "An experimental study on compliance control for a redundant personal robot arm," *Robot. Auton. Syst.*, vol. 44, pp. 101–129, 2003.

[14] L. Zollo, B. Siciliano, A. De Luca, *et al.*, "Compliance control for an anthropomorphic robot with elastic joints: Theory and experiments," *J. Dyn. Sys., Meas., Control*, vol. 127, pp. 321–328, 2005.

[15] D. Formica, L. Zollo, and E. Guglielmelli, "Torque-dependent compliance control in the joint space of an operational robotic machine for motor therapy," *J. Dyn. Sys., Meas., Control*, vol. 128, pp. 152–158, 2006.

[16] E. Lopez, K.-W. Kwok, C. J. Payne, *et al.*, "Implicit Active Constraints for Robot-Assisted Arthroscopy," in *IEEE ICRA 2013*, 2013, p. Paper Accepted.

[17] L.N. Verner and A.M. Okamura, "Force and torque feedback vs force only feedback,"in *World Haptics 2009*, 2009, pp. 406 – 410.

[18] G. Schreiber, A. Stemmer, and R. Bischoff, "The Fast Research Interface for the KUKA Lightweight Robot," in *IEEE ICRA 2010 Workshop*, 2010, pp. 15–21.